Interaction between Zeolites and Cluster Compounds

Part 2.—Thermal Decomposition of Iron Pentacarbonyl on Zeolites

By Thomas Bein†

Institute für Physikalische Chemie der Universität Hamburg, Laufgraben 24,
D-2000 Hamburg 13, Federal Republic of Germany

and Peter A. Jacobs*

Centrum voor Oppervlaktescheikunde en Colloïdale Scheikunde,
Katholieke Universiteit Leuven, Kardinaal Mercieplaan 92, B-3030 Leuven (Heverlee),
Belgium

Thermal decomposition in a thermobalance of $Fe(CO)_5$ adsorbed on alkali-metal, hydrogen-Y, dealuminated Y, L and omega zeolites proceeds stepwise *via* slow decarbonylation at low and high temperatures, separated by a fast endothermic reaction. Average CO/Fe ratios have been determined after each step. From i.r. results the former intermediates are assigned to species bearing bridging CO, whereas reaction products with CO/Fe < 1 are associated with highly unsaturated carbonyl clusters in strong interaction with the zeolite.

The thermal stability of zeolite/$Fe(CO)_5$ adducts as well as of the intermediates increases with the electron-donor properties of the matrix and can be rationalized using the Sanderson electronegativity concept. Iron loadings ranging from 2.4 wt % in zeolite L up to 10 wt % with NaY and HY are obtained by decomposition in inert atmosphere. Under vacuum conditions loss of metal up to 50% is observed. Metallic iron clusters are the final decomposition products in alkali-metal zeolites, as probed by NO adsorption. In HY part of the metallic iron is oxidized to Fe^{II} ions, which are located at cation positions.

Attempts to prepare a mononodal metal particle-size distribution on zeolites need no further justification, since these materials may have unusual properties in metal catalysis. This is certainly true for Fe zeolites, which by such classical methods of preparation as hydrogen or sodium vapour reduction of iron(II)-exchanged samples show multinodal distributions and/or chemically contaminated metal phases.[1–3] In the present work the thermal decomposition of sorbed iron pentacarbonyl, $Fe(CO)_5$, was chosen as an alternative route. Zeolites are suitable supports as a result of their variable defined cage dimensions and cation-exchange capacity, which can be used to adjust the electronic properties.[4, 5]

In the first part of this series equilibrium sorption data of $Fe(CO)_5$ on several zeolites were reported.[6] It seems that for room-temperature sorption a critical pore diameter of *ca.* 0.67 nm is needed in order to be able to reach complete pore filling. The sorbate–zeolite matrix interaction, and consequently the packing of iron pentacarbonyl, was found to be determined mainly by the nature of the zeolite charge-compensating cations rather than by the structure of the pores.

The gas-phase decomposition of $Fe(CO)_5$ occurs stepwise. The process is initiated by a slow release of the first CO ligand followed by a fast decomposition of the species

† On leave from: Centrum voor Oppervlaktescheikunde en Colloïdale Scheikunde, Katholieke Universiteit Leuven, De Croylaan 42, B-3030 Leuven (Heverlee), Belgium.

Table 1. Unit-cell composition of the zeolites

zeolites	unit-cell composition
FAU	$Na_{55.5} Al_{55.5} Si_{136.5} O_{384}$
Cs-FAU	$Cs_{37} Na_{18.5} Al_{55.5} Si_{136.5} O_{384}$
H-FAU	$H_{50} Na_{5.5} Al_{55.5} Si_{136.5} O_{384}$
FAU*	$Si_{192} O_{384}$
LTL	$K_{8.8} Al_{8.8} Si_{27.2} O_{72}$
MAZ	$Na_{6.6} Al_{6.6} Si_{29.4} O_{72}$
MOR	$Na_8 Al_8 Si_{40} O_{96}$

formed this way. This is the result of differences in bonding energies of the CO ligands to the iron atom. The thermal decomposition of Fe(CO)$_5$ impregnated on supports is known to give a dispersed Fe^0 phase,[8] although the fate of the sorbed carbonyl during thermal decomposition is not known in detail. On thoroughly dehydroxylated MgO, adsorbed Fe(CO)$_5$ is decomposed *via* mononuclear or polynuclear species, the latter being the more thermostable.[9] Iron dodecacarbonyl, Fe$_3$(CO)$_{12}$, sorbed on the same support partially covered with surface hydroxyl groups, produced a hydridoundeca-carbonyl complex, HFe$_3$(CO)$_{11}$, which upon thermal treatment is transformed into Fe^{II} ions and superparamagnetic iron particles.[10] Partial oxidation of iron also seems to occur on other acidic supports. The evolution of molecular hydrogen on γ-alumina[11] and hydrogen-Y zeolite[12, 13] during thermal treatment of the pentacarbonyl–support adduct is considered to be evidence for this reaction.

Recently it was established using volumetric methods that the thermal decomposition of Fe(CO)$_5$ on γ-alumina[11] and of Fe$_3$(CO)$_{12}$ on NaY zeolite[14] occurs in a stepwise fashion. The same was found to be true for Fe(CO)$_5$ adsorbed on NaY or HY zeolites,[15] although on the latter support Fe$_3$(CO)$_{12}$ may be one of the early intermediates. N.m.r. methods indicate that the interaction of these intermediates with the hydrogen-Y zeolite depends upon the method used for their formation.[16]

In order to be able to prepare a mononodal iron metal particle-size distribution it was the aim of the present work to elucidate the thermal-decomposition processes of Fe(CO)$_5$ on several large-pore zeolites, either with acidic or non-acidic properties. Attention was focussed more particularly on the thermal stability of sorbed Fe(CO)$_5$, the nature and reactivity of intermediates and the influence of the zeolite itself on this behaviour. Thermoanalytical techniques were used to follow the decomposition in a quantitative way and *in situ* i.r. spectroscopy to probe the carbonyl–zeolite interactions.[6]

EXPERIMENTAL

MATERIALS

All zeolites used were of synthetic origin. The unit-cell composition of the dry zeolites was determined by atomic absorption spectrometry and is given in table 1. A mnemonic code was used to identify the structure type,[17] and the pretreatment procedures are given elsewhere in more detail.[6] NaY was from Strem Chemicals (FAU) and TMA-omega from Linde (MAZ). CsY (Cs-FAU) was obtained from NaY by ion exchange. HY (H-FAU) was obtained by thermal decomposition of NH$_4$Cl-exchanged NaY at 720 K. Dealuminated Y (FAU*) was prepared from steamed NH$_4$Y (at 820 K), subsequently treated with SiCl$_4$ vapour at 820 K and then calcined at 1220 K. Linde L (LTL) and Na-mordenite (MOR) from Norton were used without pretreatment. Before use all zeolites were stored over saturated NH$_4$Cl solution in order to ensure constant humidity.

Iron pentacarbonyl from Ventron (99.5%) was cold-distilled in the dark and stored over molecular sieve 5A.

METHODS

Thermoanalytical d.t.a. and d.t.g. measurements were made in a Mettler Thermoanalyser 2 under helium purge, mostly in the 10–1 mg range, the error of the measurements being < 0.1 mg. Samples of 10 ± 2 mg zeolite and the same amount of dried Al_2O_3 as reference were placed in Pt crucibles of 7 mm height and 4 mm diameter. The samples were degassed by heating at a rate of 2 K min^{-1} up to 720 K, keeping the temperature at this value for 10 h. Loading of the samples with $Fe(CO)_5$ proceeded at 293 K in a stream of dry helium (2.8 dm^3 h^{-1}). The partial pressure of the carbonyl was 0.4 kN m^{-2}. Thermal decomposition was also carried out in a stream of helium at the same flow rate. Before increasing the sample temperature, the samples were purged at room temperature for 1 h. The arrangement of the sample holder in the balance is such that the carrier stream is directed to the top of the crucible containing the sample but does not pass through the bed of the sample, so that sorption or desorption from the sample is governed by diffusion processes.

Weight changes of samples loaded with pentacarbonyl were also determined in McBain balances under a dynamic vacuum of 10^{-3} N m^{-2}. After contacting the sample with 0.88 kN m^{-2} of sorbate for 24 h, the samples were decarbonylated stepwise at different temperatures. Degassing was performed at 333 K for 5 h, at 373 K for 15 h, at 413 K for 22 h and at 493 K for 20 h. The heating rate applied was 0.5 K min^{-1}.

The infrared spectra were recorded with a Perkin-Elmer 580 B spectrometer in the 4000–1200 cm^{-1} range. The scan mode used provided a resolution better than 1.5 cm^{-1}. The zeolite powder was pressed to self-supporting wafers of ca. 5 mg cm^{-2} at 0.1 GN m^{-2}. A quartz cell with 80 mm path length and equipped with CaF$_2$ windows of 3 mm thickness was placed in the spectrometer and was connected to a greaseless gas dosing and handling system. The zeolite wafers were degassed in this cell at 720 K and 10^{-3} N m^{-2} for 2 h. They were loaded at 293 K with $Fe(CO)_5$ vapour as follows. The carbonyl was frozen in liquid air, outgassed and allowed to warm up until the desired pressure was reached. Ca. 10% saturation was reached after contacting the zeolite wafers with 3 N m^{-2} of $Fe(CO)_5$ for 10 s, whereas saturation was obtained by contacting the wafers with 0.88 kN m^{-2} of $Fe(CO)_5$ for 1 h. The sample loaded with pentacarbonyl was then degassed for 10 min and heated at 10 K min^{-1} after addition of 60 kN m^{-2} of helium to the cell.

RESULTS AND DISCUSSION

VACUUM DECOMPOSITION OF IRON PENTACARBONYL–ZEOLITE ADDUCTS

Representative weight-loss curves of zeolites, loaded with $Fe(CO)_5$ at room temperature, during thermal treatment *in vacuo* are given in fig. 1. These data obtained in a McBain balance show that for LTL, MAZ and FAU zeolites the greatest weight loss occurs between 330 and 370 K and the decomposition is complete around 420 K. H-FAU and MOR samples behave in a similar way. The colour of the samples becomes grey or black depending on the degree of iron loading. Upon further heating to 600 K, in no case was a decrease in weight found. This proves that the zeolite heated until 420 K is always CO-free. Fig. 1 also shows that the steady weight obtained for LTL and MAZ corresponds within the experimental error to the weight expected when all the sorbed $Fe(CO)_5$ is decarbonylated. It can be shown that for FAU zeolites 25% of the iron is sublimated from the sample, while for H-FAU and MOR iron losses of 50% occur. If decomposition is carried out in a continuous-flow reactor using a purge of an inert gas, a similar loss of iron is found. Iron loadings varying between 1 and 8 wt% have been reported using thermal vacuum decomposition of $Fe(CO)_5$–HY adducts,[13, 16] which confirms that iron loss is extremely dependent on the decomposition procedure used. Obviously the one-dimensional channel structure of MAZ and LTL zeolites prevents extensive loss of iron. Since the free diameter of the pores in MAZ
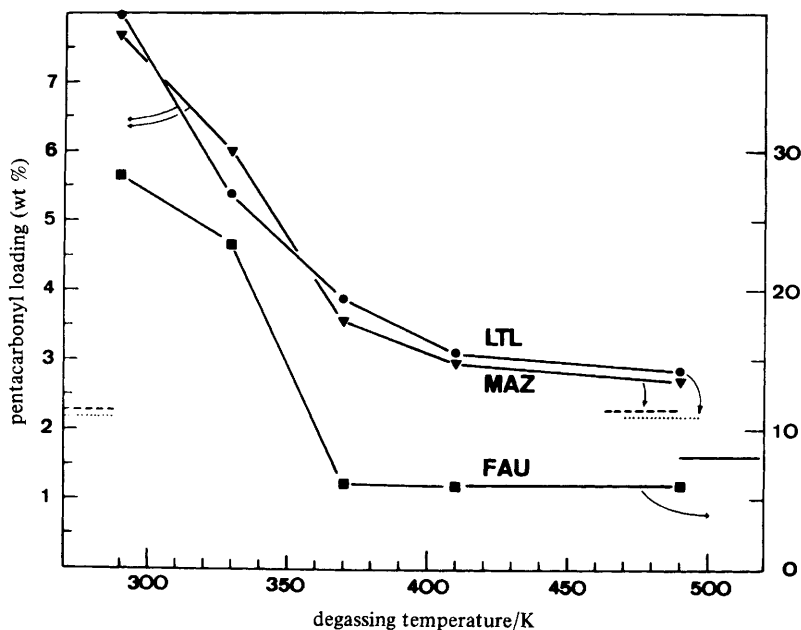
Fig. 1. Weight-loss curves upon thermal decomposition under vacuum in a McBain balance of zeolites loaded with $Fe(CO)_5$. The horizontal lines represent the theoretical levels in the case that no iron is lost during desorption.

and LTL zeolites only slightly exceeds the kinetic diameter of the sorbate, reduced mobility and effective pore-mouth blocking seems to hinder the loss of $Fe(CO)_5$ during the decomposition procedure.

DECARBONYLATION OF $Fe(CO)_5$–ZEOLITE ADDUCTS IN A THERMOBALANCE

The thermoanalytical changes occurring during heating of $Fe(CO)_5$–zeolite adducts are shown in fig. 2 (A) for the FAU and Cs-FAU samples and in fig. 2 (B) for the H-FAU and FAU* zeolites. In every case an endotherm d.t.a. effect occurs which is accompanied by a relatively fast decrease in sample weight. For FAU and Cs-FAU samples [fig. 2(A)] the sample weight starts to decrease slowly but then suddenly drops when the endothermic process occurs. After this endothermic event the decarbonylation again proceeds slowly, as can be seen from the slow decrease in weight. As shown in table 2, MAZ and LTL behave similarly.

The H-FAU and FAU* matrices [fig. 2(B)] show different behaviour. On these samples the decarbonylation is complete when the endothermic reaction has stopped. On FAU*, the rate of weight loss increases gradually and a distinction between the slow and fast decarbonylation processes can only be made formally. With H-FAU a very broad endotherm is found in which two steps can be distinguished. When the characteristic d.t.a. temperatures (T_i, T_m and T_f are the temperatures at which the d.t.a. peak starts, is at its maximum and ends, respectively) and the temperatures at which decarbonylation is complete are compared for the faujasite-type zeolites (table 2), the following sequence for the stability of sorbed $Fe(CO)_5$ as well as for the intermediates is obtained:

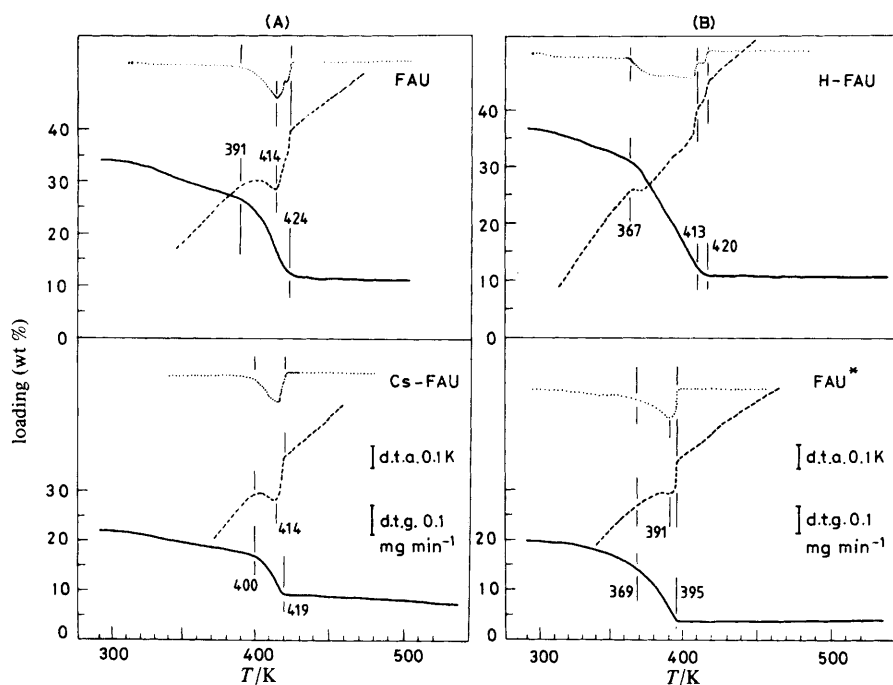$$FAU* < H\text{-}FAU < FAU < Cs\text{-}FAU.$$
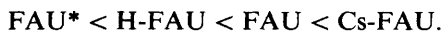
Fig. 2. Thermogram of the decarbonylation of $Fe(CO)_5$–zeolite adducts performed at a heating rate of 2 K min^{-1}: (——) weight-loss curve, (...) d.t.g. signal; (— — —) d.t.a. endotherm.

Table 2. Characteristic temperatures during thermoanalysis^a of $Fe(CO)_5$–zeolite adducts

	d.t.a. endotherm			T/K at which constant weight is reached (T_c)
zeolite	T_i/K (start)	T_m/K (peak)	T_f/K (end)	
FAU	391	414	424	553
Cs-FAU	400	414	419	573
H-FAU	367	380^b 400^b	420	420
FAU*	369	391	395	395
LTL	383	(420)^c	448	563
MAZ	363	378	383	443

^{a} With 10 ± 2 mg of sample, using a heating rate of 2 K min^{-1}. ^{b} Broad endotherm consisting of two ill-defined maxima. ^{c} Very weak endotherm.

Since the cage dimensions are almost similar in these samples, it seems that the nature of the cation determines the stability of the unperturbed as well as the partially decomposed $Fe(CO)_5$–zeolite adducts.

A comparison of the LTL and MAZ structures indicates higher stability for the LTL–carbonyl adduct (table 2). This may be the effect of the charge-compensating
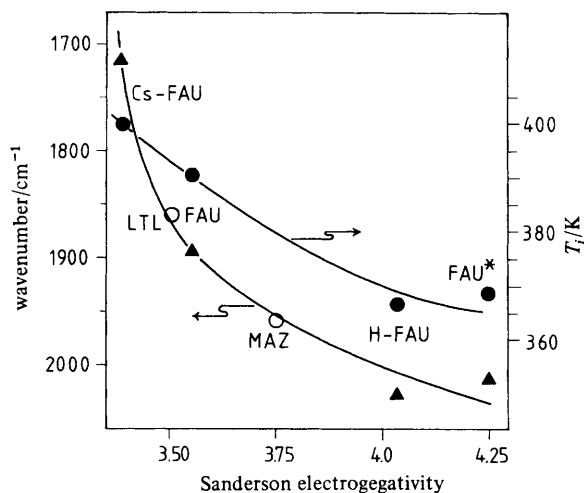
Fig. 3. Correlation between the Sanderson electronegativity of the zeolite and (*a*) the temperature T_i at which the fast decarbonylation of the $Fe(CO)_5$–zeolite adduct starts (●) and (*b*) the stretching frequency of residual CO ligands after almost complete decarbonylation of the adduct (▲).

cation (K in LTL as against Na in MAZ) or of the smaller pore diameter in the LTL structure, which may result in a more effective pore mouth blocking. In order to quantify the influence of changes in the chemical composition of the zeolites, the characteristic temperatures of the d.t.a. endotherm have been correlated with their average electronegativity calculated according to Sanderson.[18, 19] There is now ample evidence in the literature that variation in zeolite properties can be explained reasonably well and even predicted using this formalism.[4, 5, 20] As an example, in fig. 3(*a*) a correlation between T_i and the Sanderson electronegativity is shown to hold for the homologous series of FAU structures, while values for LTL and MAZ deviate. Two effects emerge which seem to determine the stability of the adduct: the chemical composition of the zeolite and the size and geometry of the zeolite channels. For the FAU series the stability of the adducts decreases with decreasing basicity of the samples. A more extensive discussion on this will be found in the discussion of the i.r. results.

Iron loadings obtained after complete decomposition of the adducts (table 3) range from 1 to 10 wt %. For the FAU samples, the loading is *ca.* 10%, except for FAU* on which a significant loss of carbonyls is found during the heat treatment. The iron loadings on the other structures (2.4% on MAZ, 2.8% on LTL and 1% on MOR) are sufficiently high to use the iron for catalytic applications.

INTERMEDIATES FORMED UPON THERMAL ACTIVATION OF $Fe(CO)_5$–ZEOLITE ADDUCTS

From table 3 it also follows that, for the decomposition procedures used, the samples lose the same relative amounts of carbonyl at the specific temperatures determined by the endothermic effect. During the pre-endothermic period, *i.e.* before the characteristic endotherm is observed, most samples lose 20–30% of total sorbate weight. At the end of the endotherm between 60 and 70% has disappeared. When complete decarbonylation has occurred the residual iron on the samples is between

Table 3. Decarbonylation of $Fe(CO)_5$–zeolite adducts in a thermobalance:[a] (a) the fraction (F) of the original loading remaining adsorbed at the characteristic d.t.a. temperatures (T_i, T_f and T_c); (b) the average stoichiometries (X) of $[Fe(CO)_x]_y$ formed during decarbonylation at the characteristic d.t.a. temperatures

sample	T_i		T_f		T_c		iron loading[b] (wt %)
	F	X	F	X	F	X	
FAU Ca-	68	2.8	33	0.3	29	0.0	9.7 ± 0.7
FAU	74	3.2	37	0.6	26	-0.2	5.8
FAU$^+$	—	—	—	—	13	—	2.0
LTL	72	3.2	35	0.4	27	-0.1	2.8
MAZ	81	3.7	42	0.9	33	0.3	2.4
H-FAU	86	4.0	38	0.7	31	0.2	10.5

[a] With 10 ± 2 mg of sample, using a heating rate of 2 K min^{-1}. [b] Iron metal per weight of dry zeolite after complete decarbonylation. [c] Taken at the end of the first endotherm at 413 K [see fig. 2(b)].

26 and 33% of the original weight of sorbate. Only sample FAU* behaves exceptionally, since not only CO but also an important amount of iron is lost. The data presented allow us to state the following.

(1) During a thermoanalytic experiment, $Fe(CO)_5$ sorbed on zeolites can be decarbonylated without any detectable loss of iron. Only on a dealuminated Y zeolite is iron loss significant during this treatment. Note that during vacuum decomposition of the carbonyl, iron loss is always important.

(2) Decarbonylation occurs stepwise on the alkali-metal-cation-exchanged zeolites. On average, $[Fe(CO)_3]_m$ species are formed during a slow decomposition step. A subsequent fast reaction transforms these species to $[Fe(CO)_x]_n$ intermediates. x is between 0.3 and 0.8 and m and n represent respective nuclearity. Detailed average stoichiometries for the intermediates $[Fe(CO)_x]_y$ can be derived from the data of table 3(a) using the relation indicated. The results are given in table 3(b).

(3) The H-FAU–carbonyl adduct behaves differently compared to the zeolites containing alkali-metal cations. The first slow release of one CO ligand per atom of iron is followed by two fast endothermic processes, involving the removal of $ca.$ three and one CO ligands per Fe, respectively.

From the homogeneous gas-phase decomposition of iron pentacarbonyl, it was derived that the first Fe—C bond scission should be rate determining.[7] Its bond energy amounts to 201 kJ mol^{-1}, which exceeds by far the average Fe—C bond energy of 117 kJ mol^{-1}.[7] These results, as well as those from a recent study of the laser-induced photodissociation of $Fe(CO)_5$ vapour,[21] provide evidence for a non-statistical decomposition process. The Fe—C bond strength of the $Fe(CO)_x$ intermediates, determined using laser photoelectron spectrometry,[22] are 2.4, 0.2, 1.4 and 1 eV for $Fe(CO)_5$, $Fe(CO)_4$, $Fe(CO)_3$ and $Fe(CO)_2$, respectively. This implies that decomposition of $Fe(CO)_5$ vapour occurs via a slow removal of the first CO ligands. Essentially the same is observed in the present work for $Fe(CO)_5$ adsorbed on zeolites.

On the contrary, thermogravimetric and i.r. results indicate that no such intermediates exist when Fe_3CO_{12} in a KBr matrix is thermally decomposed.[23] On NaY zeolite,

however, iron dodecacarbonyl decomposition also seems to occur stepwise, as shown by i.r. spectroscopy and temperature-programmed desorption.[14] The following values of x are observed at the temperatures indicated:

$$4 \xrightarrow{\text{343 K}} 2.8 \xrightarrow{\text{388 K}} \ll 1.2 \xrightarrow{\text{423–473 K}} 0.$$
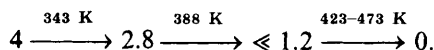
The release of 1.2 CO per Fe was associated with the occurrence[14] of a dismutation reaction of $Fe_3(CO)_{12}$ into Fe^{2+} and $Fe_3(CO)_{11}^{2-}$ ions instead of a simple decarbonylation reaction. Although the sequence for the values of x closely resembles the sequence obtained in this work for decomposition of $Fe(CO)_5$ on alkali-metal-cation zeolites, including faujasite, the dismutation reaction is discarded for reasons explained below.

The thermal decomposition of $Fe(CO)_5$ on γ-alumina under a flow of inert gas was also followed using temperature-programmed desorption.[11] In this way iron losses up to 50%, and as a result low Fe^0 loadings (up to 0.3 wt %), are found. The number of ligands (x) per Fe were found to vary as follows:

$$5 \xrightarrow[\text{fast}]{} 2 \xrightarrow[\text{slow}]{} 0.$$
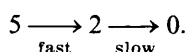
Evolution of CO started at 333 K, reached a maximum at 413 K and slowly continued up to 670 K.

It may be concluded from all these results that the decomposition of iron carbonyls, supported or not, starts with slow evolution of a few CO ligands, followed by fast release of the major part of the ligands. With most support materials, complete removal of residual CO occurs only slowly. Sensitive monitoring of the accompanying thermal processes is needed to detect these stepwise variations in the number of CO ligands. This is most probably the reason why different authors sometimes obtain conflicting data.

APPARENT ACTIVATION ENERGY FOR DECOMPOSITION OF $Fe(CO)_5$ ON FAU

From the variation of the temperature at which a d.t.a. maximum occurs with the heating rate, the apparent activation energy of the process can be determined,[24] provided the volume of the sample cell is small and the reaction rate is moderate.[25] This was true for the present experiment. When the heating rate was varied between 0.2 and 2 K min^{-1} an apparent activation energy of 100 ± 20 kJ mol^{-1} was calculated for the decomposition of $Fe(CO)_5$ on FAU in the temperature region of the d.t.a. endotherm. From deposition experiments of $Fe(CO)_5$ on steel,[26] a value of 84 kJ mol^{-1} was found for the apparent activation energy of pentacarbonyl decomposition. For $Fe(CO)_5$ on γ-alumina a value of 126 kJ mol^{-1} could be determined.[11] It seems that the apparent activation energy of $Fe(CO)_5$ decomposition is independent of the substrate and represents for a major part the slowest step, namely the initial release of two CO ligands. The value obtained differs significantly from the dissociation energy reported for the removal of the first ligand from gaseous $Fe(CO)_5$, i.e. 201 kJ mol^{-1}.[7] Since decomposition of $Fe(CO)_5$ starts at 333 K in contact with metallic iron,[27] an autocatalytic step seems to be involved in this reaction. This is confirmed by t.p.d. results.[11]

I.R. INVESTIGATION OF THE THERMAL DECOMPOSITION OF IRON PENTACARBONYL–ZEOLITE ADDUCTS

In situ thermal decomposition of the adducts was carried out in a static helium atmosphere. The spectral changes in the CO-stretching region were recorded systematically during decarbonylation. Representative spectra for the adducts of $Fe(CO)_5$ with FAU, Cs-FAU, LTL and H-FAU zeolites are shown in fig. 4–7, respectively.
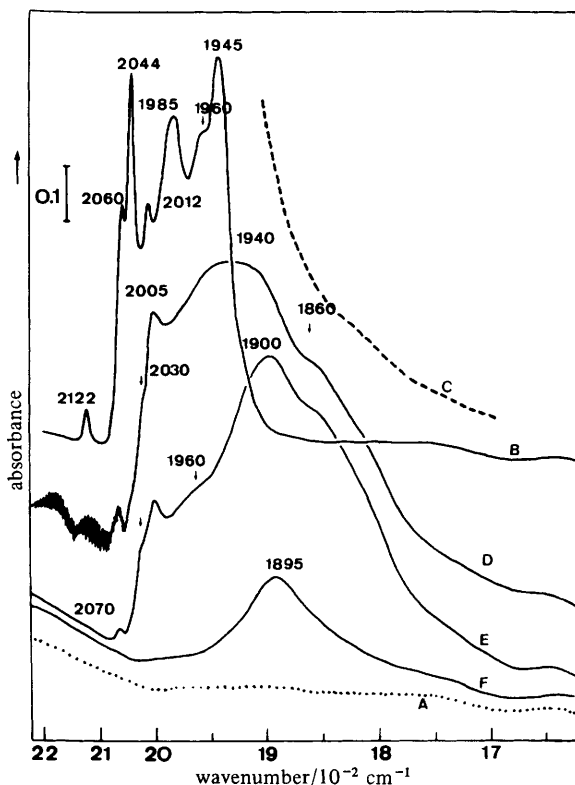
Fig. 4. I.r. spectra of the CO-stretching region during decarbonylation in inert atmosphere of Fe(CO)$_5$–FAU adducts: (A) FAU zeolite degassed at 720 K, (B) the adduct at 10% saturation, (C) the saturated adduct heated at 373 K for 15 min in 60 kN m^{-2} of helium, (D) heated at 420 K for 15 min under helium, (E) vacuum degassed at 420 K, (F) heated at 470 K for 70 min after introduction of the same amount of helium.

BEHAVIOUR OF ALKALI-METAL-CATION ZEOLITES

During the decomposition of Fe(CO)$_5$ on the zeolites FAU, Cs-FAU and LTL (fig. 4–6) the original CO-stretching bands of the adduct in the region of linearly bound CO gradually decrease in intensity, while in the region of bridged CO (below 1900 cm^{-1}) the i.r. absorption increases. The latter bands are found at 1860 cm^{-1} for FAU, at 1875 cm^{-1} for LTL and at 1818 cm^{-1} for Cs-FAU. As a result of their intermediate appearance in the decomposition process, these bands can be associated with the existence of the [Fe(CO)$_3$]$_m$ fragments evidenced by the d.t.a. experiments. The question arises as to whether cluster formation occurs already with these fragments prior to complete decarbonylation. The CO-stretching bands in the frequency range below 1900 cm^{-1} can alternatively be assigned to bridged CO ligands or anionic carbonyl species, respectively.

The interpretation of the data presented by assuming bridged CO is preferred for the following reasons. (i) Formation of anionic species in dehydrated alkali-metal zeolite would require a dismutation reaction providing cations such as Fe^{2+}. These have never been detected after complete decomposition of the adducts. (ii) Assuming
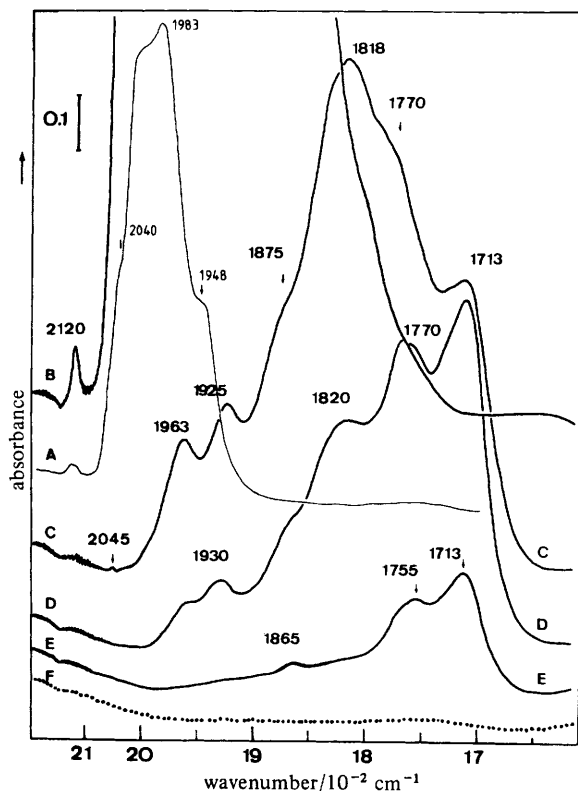
Fig. 5. Spectra of CO stretching for the Fe(CO)$_5$–Cs-FAU adduct: (A) the adduct at 10% saturation, (B) the saturated adduct heated up to 400 K in helium, (C) heated at 470 K for 40 min, (D) at 470 K for 2 h, (E) degassed at 720 K.

the intermediate formation of anionic species, it would be difficult to explain the ultimate generation of Fe^0 particles after complete decomposition as observed by magnetic measurements.[39] (iii) With a localized negative charge on a certain inter-mediate, the striking influence of the zeolite cations on the CO-stretching frequencies would also be difficult to explain (see below).

However, only complementary experiments such as *in situ* magnetic measurements would rule out completely the assignment of the low-frequency bands to anionic mononuclear complexes.[40] In analogy to the d.t.a. results the bands which remain on these zeolites at relatively high temperatures must be assigned to highly unsaturated [Fe(CO)$_x$]$_n$ species, with an average stoichiometry of $x = 0.5$. These bands are seen at 1895, 1875 and 1713 cm^{-1} for FAU, LTL and Cs-FAU, respectively. Although the bands for Cs-FAU are in a region where surface carbonate or carboxylate species absorb,[28, 29] they cannot be assigned to these species, since the vibrations expected in the 1500–1300 cm^{-1} range are not observed. An explanation for the influence of the nature of the matrix on the frequency of these bands will be advanced below. MAZ and MOR zeolites adsorb only a limited amount of Fe(CO)$_5$. Upon decomposition, these adducts are expected to behave in the same way as FAU, although this could not be verified owing to the low intensity of the residual CO bands. The existence of a dismutation reaction of Fe$_3$(CO)$_{12}$ adsorbed on FAU has been invoked[14] during
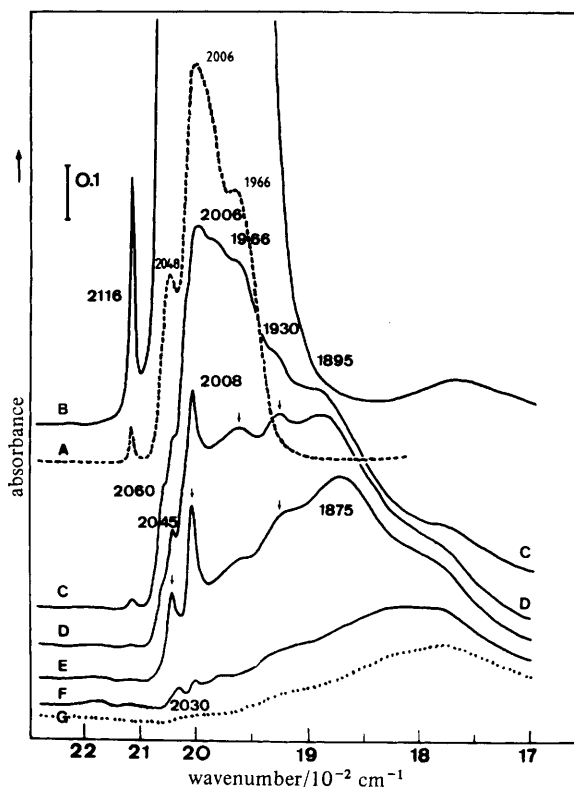
Fig. 6. I.r. spectra of the decarbonylation of $Fe(CO)_5$–LTL: (A) the adduct at 10% saturation, (B) saturated adduct in helium, (C) heated at 420 K for 1 h, (D) for 2 h, (E) heated at 470 K for 30 min, (F) heated up to 550 K, (G) degassed at 720 K.

moderate heating at 333 K. Evidence for this reaction was based only on the similarity of the CO stretching frequencies of the expected dismutation product $[Fe_3(CO)_{11}]^{2-}$ and the heated $Fe_3(CO)_{12}$–FAU adduct, respectively. For the following two reasons this assumption is questionable: (i) the assignment of some of the carbonyl bands observed to particular species such as $[Fe_3(CO)_{11}]^{2-}$ is arbitrary, since the CO-stretching patterns of carbonyl complexes are sensitive to solvent effects[14] and often are found in the frequency region considered here; (ii) Fe^{2+} ions, which are expected as the other dismutation product, have been observed neither after decomposition of a $Fe_3(CO)_{12}$–FAU adduct[14] nor after decomposition of a $Fe(CO)_5$–FAU adduct (this work).

BEHAVIOUR OF THE CATION-FREE FAUJASITE

Upon decomposition of the FAU*–$Fe(CO)_5$ adduct, the i.r. bands in the CO-stretching region gradually decrease in intensity and only minor frequency shifts and changes in peak intensities occur. It has already been concluded[6] that in this adduct only a small interaction exists between matrix and sorbate. This explains why the major amount of carbonyl is desorbed upon heating. The $[Fe(CO)_3]_m$ intermediates are not formed, since stabilisation by the matrix is lacking.

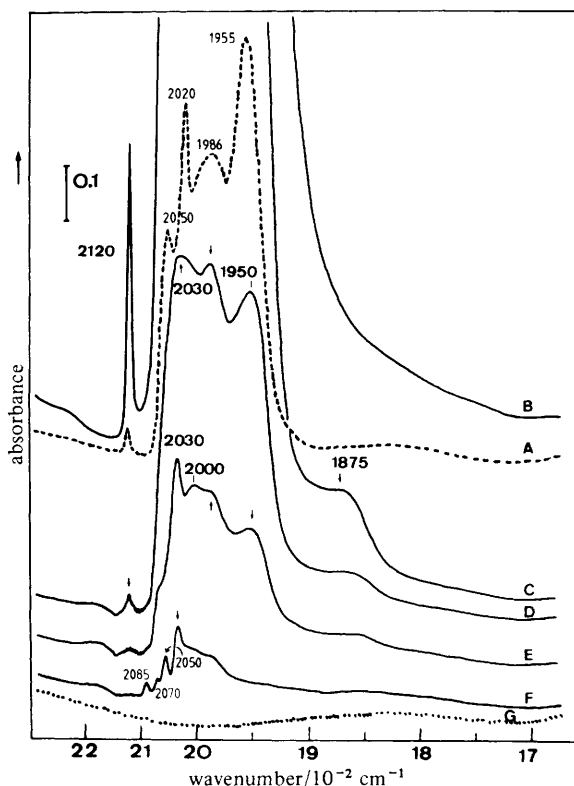**Fig. 7.** I.r. spectra of the decarbonylation of Fe(CO)$_5$–H-FAU: (A) the adduct at 10% saturation, (B) the saturated adduct, (C) heated in helium at 400 K for 10 min, (D) for 25 min, (E) for 32 min, (F) for 16 h at 400 K, (G) degassed at 720 K.

BEHAVIOUR OF ACIDIC FAUJASITE

Upon decomposition of the H-FAU–carbonyl adduct, most of the broad low-frequency CO bands which are found for the cationic forms of this zeolite are not generated (fig. 7). Only one new band at 1875 cm^{-1}, of minor intensity, appears in this frequency range during the decomposition process. This low-frequency band disappears even faster than the bands around 2000 cm^{-1}. The low number and low thermal stability of the CO bands provide evidence for another but simpler decomposition pattern. The intermediate formation of Fe$_3$(CO)$_{12}$ has been postulated in this case.[13, 15]

Inspection of the OH region during adduct decomposition provides supplementary evidence for this mechanism (fig. 8). Upon adsorption a hydrogen bond of moderate strength is formed with all protons available in the supercage: the 3645 cm^{-1} band shifts to 3550 cm^{-1}. After complete decarbonylation both the 3645 and 3550 cm^{-1} bands are only partially restored [fig. 8(C)], which indicates that deprotonation of the lattice has already occurred at these low temperatures. The extent to which this occurs depends very much on the decomposition conditions. After heating at 420 K for 45 min almost 75% of the original intensity is restored [fig. 8(C)], while after prolonged heating at 400 K for 960 min only 25% of the OH groups resist [fig. 8(D)]. The extent
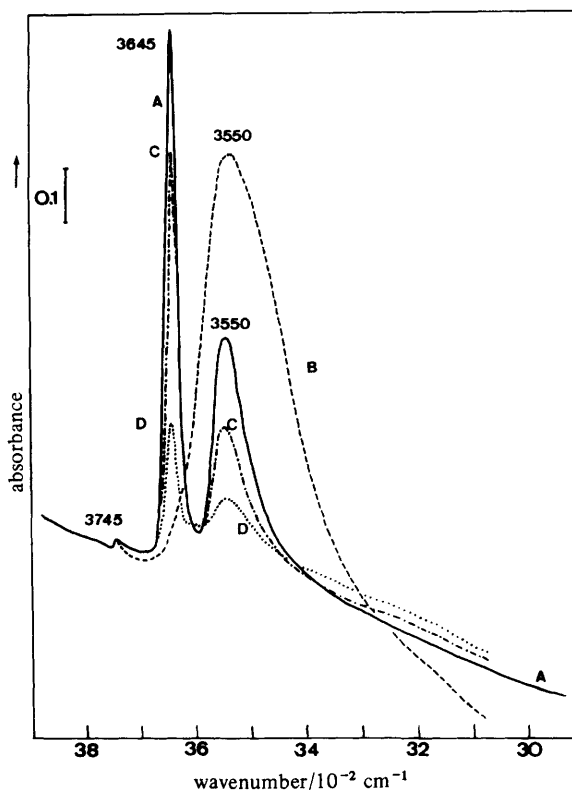
Fig. 8. Interaction of the OH groups of H-FAU with $Fe(CO)_5$: (A) OH groups after degassing at 720 K, (B) saturation with $Fe(CO)_5$, (C), the adduct heated at 420 K for 45 min, (D) the adduct heated at 400 K for 16 h.

to which the OH groups disappear is a measure of the amount of Fe^{II} ions formed during the acid reaction. A possible reaction is the oxidation of sorbed carbonyl:[13, 30]

$$Fe(CO)_5 + 2H^+ \longrightarrow H_2 + Fe^{2+} + 5CO.$$
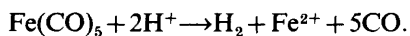
The data of fig. 8 show that this cannot be the major pathway. Indeed, after prolonged heating at a low temperature more OH groups are removed than after shorter heating at a higher temperature [fig. 8(C) and (D)]. This is only possible if the oxidation of Fe^0 clusters is a major reaction pathway:

$$Fe^0 + 2H^+ \longrightarrow H_2 + Fe^{2+}.$$
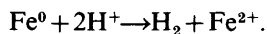
AN ATTEMPT TO RATIONALIZE THE INFLUENCE OF THE MATRIX UPON THE DECOMPOSITION OF THE ADDUCT

There is general agreement in the literature[31-34] as to the influence of the number of electron-donor ligands (L) on the frequency of the CO bands in $L_x Fe(CO)_{5-x}$. When the value of x increases, a decrease of the CO-stretching frequency is found. The increased stability of $Fe(CO)_5$ in FAU compared with H-FAU was explained by

Fig. 9. I.r. spectra of the stretching region of NO, sorbed at 293 K on decarbonylated $Fe(CO)_5$–zeolite adducts: (A) the carbonyl–LTL adduct heated at 550 K, (B) addition of NO at 293 K (10^4 N m^{-2}), (C) room-temperature degassing at 10^{-2} N m^{-2} for 10 min, (D) the carbonyl–FAU adduct heated at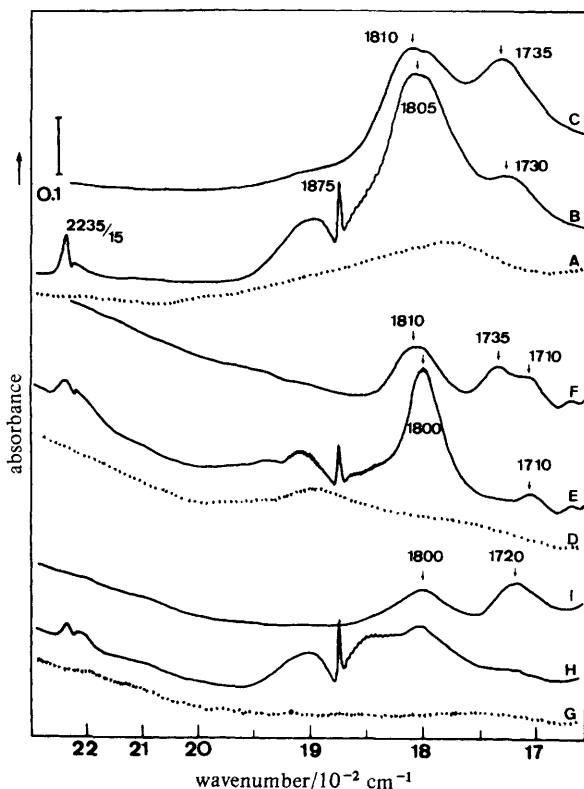 470 K, (E) the same as for (B), (F) the same as for (C), (G) the carbonyl–Cs-FAU adduct heated at 550 K, (H) the same as for (B), (I) the same as for (C).

increased backbonding in the Fe—CO bond, resulting from increased electron-donor properties of the matrix.[15] This hypothesis is confirmed in the present work. Indeed a monotonous correlation exists between the Sanderson electronegativity of the zeolite and the thermal stability of the adducts [fig. 3(a)]. When the zeolite–$Fe(CO)_5$ adduct is more stable, the CO frequencies are found at lower wavenumbers. Another monotonic correlation is established between the CO frequencies and the Sanderson electronegativity values of the zeolite [fig. 3(b)]. It follows that when the overall electron-donor properties of the zeolite matrix (as determined by their overall chemical composition) increase, the corresponding CO-stretching vibrations of the $[Fe(CO)_x]_y$ intermediates are found at lower wavenumbers.

PROBING OF THE DECARBONYLATED ADDUCTS WITH NO

Upon room-temperature addition of NO (10 kN m^{-2}) to the decarbonylated adducts of iron pentacarbonyl and the alkali-metal-cation-exchanged zeolites (LTL, FAU and Cs-FAU), spectra of remarkable similarity are observed (fig. 9). Apart from the stretching frequency of gas-phase NO at 1875 cm^{-1}, two typical bands are
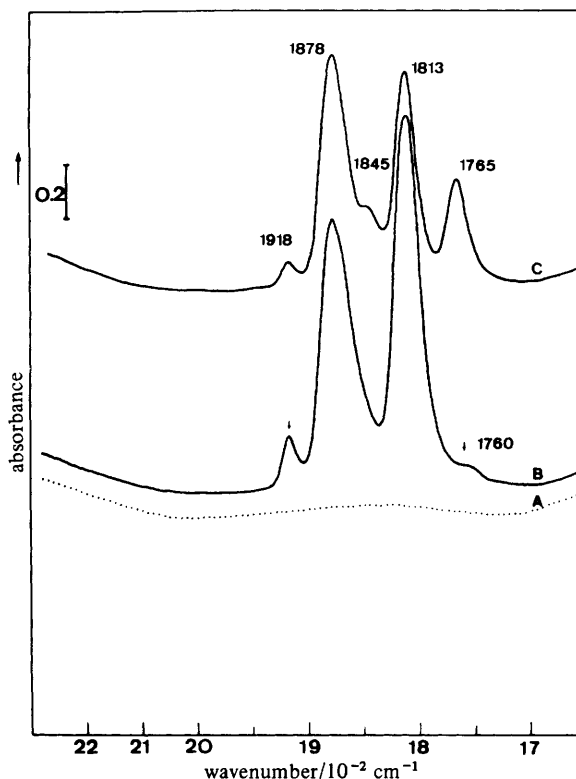
Fig. 10. I.r. spectra of NO adsorbed at 293 K on a decarbonylated $Fe(CO)_5$–H-FAU adduct: (A) the adduct heated at 430 K, (B) addition of NO at 293 K (10^4 N m^{-2}), (C) room-temperature degassing at 10^{-2} N m^{-2} for 10 min.

observed, between 1810 and 1800 cm^{-1} and between 1735 and 1710 cm^{-1}. Bands at 1810 and 1720 cm^{-1} with the same relative intensities have been reported for NO chemisorbed on Fe suspended in oil.[35] The assignment of the two bands has been firmly established:[36] NO chemisorbed on metallic iron absorbs at 1720 cm^{-1}, while the band around 1800 cm^{-1} is assigned to NO sorbed on surface-oxidized iron particles. It is evident that since in zeolites NO disproportionation was reported,[37] the surface of the iron phase may be oxidized by N_2O formed this way. The spectra of NO sorbed on the Fe/H-FAU system are given in fig. 10. The most significant peaks are at 1878, 1813 and 1765 cm^{-1}. Comparable spectra were obtained with H-FAU–iron dodecacarbonyl adducts.[13]

Based on earlier work[38] on Fe-Y zeolites, the 1878 and 1765 cm^{-1} bands have been assigned to [Fe(NO)]$^{2+}$ complexes of high and low spin, respectively. The band at 1813 cm^{-1} was assigned[13] to NO sorbed on FeO, which is in agreement with the present interpretation for the 1800 cm^{-1} band on alkali-metal-cation zeolites. This assignment allows us to conclude the following with regard to the nature of the Fe after decomposition of the adducts. (i) On H-FAU a considerable amount of Fe^{II} is located in cationic positions (high- and low-spin complexes with NO) as a result of the oxidation of the metal phase and irreversible removal of the acidic protons. This phenomenon is absent on alkali-metal-cation zeolites since no Brønsted-acid sites are

present. (ii) The surface of the remaining iron cluster on H-FAU is easily oxidizable by NO at room temperature, while this is only partially true for Fe clusters on alkali-metal-cation zeolites. The present data do not permit an explanation of this difference. (iii) The interaction of NO with iron clusters is stronger than with surface-oxidized clusters; this becomes evident when spectra B and C, E and F, H and I (fig. 9) are compared.

CONCLUSIONS

The combined use of thermogravimetric and i.r. methods allows one to depict the decomposition of Fe(CO)$_5$–zeolite adducts as a stepwise decarbonylation reaction, consisting of slow (s) and fast (f) phenomena.

For alkali-metal zeolites of different structure it occurs as follows:

$$\text{Fe(CO)}_5 \xrightarrow{\text{s}} [\text{Fe(CO)}_3]_m \xrightarrow{\text{f}} [\text{Fe(CO)}_{0.5}]_n \xrightarrow{\text{s}} [\text{Fe}^0]_o.$$

For HY zeolites the following sequence emerges:

$$\text{Fe(CO)}_5 \xrightarrow{\text{s}} [\text{Fe(CO)}_4]_p \xrightarrow{\text{f}} [\text{Fe(CO)}_{0.7}]_q \xrightarrow{\text{f}} [\text{Fe(O)}]_v.$$
$$\diagdown{\scriptstyle s} \quad {\scriptstyle s}\diagup$$
$$\text{Fe}^{\text{II}}$$

The fast phenomena are endothermic, characterized by an apparent activation energy of 100 ± 20 kJ mol^{-1}. I.r. results show that the intermediates cannot be exclusively of a mononuclear nature. The stability of the Fe(CO)$_x$ intermediates as well as their CO-stretching frequency increases with the electron-donor properties of the substrate, in this way enhancing the Fe—CO bond strength through increased backbonding. Use of NO as probe indicates that in H-faujasites Fe$^{\text{II}}$ ions can take cationic positions and remove the acidic protons.

[1] Y-Y. Huang and J. R. Anderson, *J. Catal.*, 1975, **40**, 143.

[2] F. Schmidt, W. Gunsser and J. Adolph. *ACS Symp. Ser.*, 1977, **40**, 291.

[3] W. Gunsser, J. Adolph and F. Schmidt, *J. Magn. Magn. Mater.*, 1980, **15–18(II)**, 1115.

[4] W. J. Mortier, *J. Catal.*, 1978, **55**, 138.

[5] P. A. Jacobs, W. J. Mortier and J. B. Uytterhoeven, *J. Inorg. Nucl. Chem.*, 1978, **40**, 1919.

[6] Th. Bein and P. A. Jacobs, *J. Chem. Soc., Faraday Trans. 1*, 1983, **79**, 1819.

[7] G. P. Smith and R. M. Laine, *J. Phys. Chem.*, 1981, **85**, 1620.

[8] A. Terenin and L. Roev, *Spectrochim. Acta*, 1959, **11**, 946.

[9] E. Guglielminotti, A. Zecchina, F. Boccuzzi and E. Borello, in *Growth and Properties of Metal Clusters*, ed. J. Bourdon (Elsevier, Amsterdam, 1980), p. 165.

[10] F. Hugues, B. Besson, P. Bussiere, J. A. Dalmon, J. M. Basset and D. Olivier, *Nouv. J. Chim.*, 1981, **5**, 207.

[11] A. Brenner and D. A. Hucul, *Inorg. Chem.*, 1979, **18**, 2836.

[12] D. Ballivet-Tkatchenko, G. Coudurier, H. Mozzanega and I. Tkatchenko, in *Fundamental Research in Homogeneous Catalysis*, ed. M. Tsutsui (Plenum Press, New York, 1979), vol. 3, p. 257.

[13] D. Ballivet-Tkatchenko and G. Coudurier, *Inorg. Chem.*, 1979, **18**, 558.

[14] D. Ballivet-Tkatchenko, G. Coudurier and Nguyen Duc Chau, in *Metal Microstructures in Zeolites*, ed. P. A. Jacobs, P. Jirü, N. Jaeger and G. Schulz-Ekloff (Elsevier, Amsterdam, 1982), p. 123.

[15] Th. Bein, P. A. Jacobs and F. Schmidt, in *Metal Microstructures in Zeolites*, ed. P. A. Jacobs, P. Kirü, N. Jaeger and G. Schulz-Ekloff (Elsevier, Amsterdam, 1982), p. 111.

[16] J. B. Nagy, M. Van Eenoo and E. G. Derouane, *J. Catal.*, 1979, **58**, 230.

[17] D. H. Olson and W. M. Meier, *Altas of Zeolite Structure Types* (IZA, Polycrystal Book Service, Pittsburgh, 1978).

[18] R. T. Sanderson, *J. Coll. Sci. Teach.*, 1972, **1**, 16; 47.

[19] R. T. Sanderson, *Chemical Bonds and Bond Energy* (Academic Press, New York, 2nd edn, 1976).

[20] P. A. Jacobs, *Catal. Rev. Sci. Eng.*, 1982, **24**, 415.

[21] J. T. Yardley, B. Gitlin, G. Nathanson and A. M. Rosan, *J. Chem. Phys.*, 1981, **74**, 370.

[22] P. C. Engelking and W. C. Lineberger, *J. Am. Chem. Soc.*, 1979, **101**, 5569.

[23] R. Psaro, A. Fusi, R. Ugo, J. M. Basset, A. K. Smith and F. Hugues, *J. Mol. Catal.*, 1980, **7**, 511.

[24] H. E. Kissinger, *Anal. Chem.*, 1957, **29**, 1702.

[25] K. Akita and M. Kase, *J. Phys. Chem.*, 1968, **72**, 906.

[26] H. E. Carlton and J. H. Oxley, *AIChE J.*, 1965, **11**, 79.

[27] A. Mittasch, *Z. Angew. Chem.*, 1928, **41**, 831.

[28] P. A. Jacobs, F. H. Van Cauwelaert, E. F. Vansant and J. B. Uytterhoeven, *J. Chem. Soc., Faraday Trans. 1*, 1973, **69**, 1056.

[29] P. A. Jacobs, F. H. Van Cauwelaert and E. F. Vansant, *J. Chem. Soc., Faraday Trans. 1*, 1973, **69**, 2130.

[30] J. Dewar and H. O. Jones, *Proc. R. Soc. London*, 1905, **76**, 569.

[31] M. Bigorgne, *J. Organometal. Chem.*, 1970, **24**, 211.

[32] B. F. G. Johnson, J. Lewis and M. V. Twigg, *J. Chem. Soc., Dalton Trans.*, 1974, 241.

[33] M. Poliakoff, *J. Chem. Soc., Dalton Trans.*, 1974, 210.

[34] P. Poliakoff and J. J. Turner, *J. Chem. Soc., Dalton Trans.*, 1974, 2276.

[35] C. Blyholder and M. C. Allen, *J. Phys. Chem.*, 1965, **69**, 3998.

[36] H. Bandow, T. Onishi and K. Tamaru, *Chem. Lett. (Jpn)*, 1978, 83.

[37] C. C. Chao and J. H. Lunsford, *J. Am. Chem. Soc.*, 1971, **93**, 71.

[38] J. W. Jermyn, T. J. Johnson, E. F. Vansant and J. H. Lunsford, *J. Phys. Chem.*, 1973, **77**, 2964.

[39] F. Schmidt, Th. Bein, U. Ohlerich and P. A. Jacobs, *Proc. Sixth Int. Zeolite Conf.*, Reno 1983 (Butterworth Scientific Press, Sevenoaks, 1983, in press).

(PAPER 3/635)